

Chapter 2

Climate Change Risks to Water Security in Canada's Western Interior



M. Rehan Anis, Yuliya Andreichuk, Samantha A. Kerr,
and David J. Sauchyn

2.1 Introduction

Much of the impact of anthropogenic climate change on social and natural systems results from changes to regional hydrological regimes including shifts in the seasonal water balances and increases in the frequency and severity of hydroclimatic extremes (Abbott et al. 2019; Jiménez Cisneros et al. 2014; Marvel et al. 2019). Climate change impacts on water resources affect food security and economic prosperity, especially in dry climates where aridity (a negative water balance in normal years) and drought are economically and ecological limiting. The semiarid to sub-humid plains of western Canada have more than 80% of the country's agricultural land. In this region, melting snow accounts for most of the runoff and surface water supplies. A warming climate will result in decreases in the depth of the snowpack, length of the snow cover season and the proportion of precipitation falling as snow (Mudryk et al. 2018), with a corresponding reduction in end-of-season snowpack and summer water levels and streamflow (Bonsal et al. 2019).

The potential impacts of a warming climate on water availability in snow-dominated mid- and high-latitude river basins are a serious concern given that, over the past several decades, these regions have experienced some of the most rapid warming on earth (Bonsal et al. 2019). In western Canada, declining streamflow has been observed in rivers draining the eastern slopes of the central/southern Rocky Mountains, (Burn et al. 2004; Rood et al. 2005; Schindler and Donahue 2006; St. Jacques et al. 2010; Bawden et al. 2015). Snow in the Rocky Mountains is the backbone of the industrial water supply, including the source of water for irrigation of agricultural land. The bank of surplus water from wasting alpine glaciers has been mostly spent, and mass balance is shrinking quickly (Marshall et al. 2011).

M. R. Anis · Y. Andreichuk · S. A. Kerr · D. J. Sauchyn (✉)
Prairie Adaptation Research Collaborative (PARC), University of Regina, Regina, Canada
e-mail: sauchyn@uregina.ca

This paper describes research on the impact of climate change on water security in western Canada using as a case study the North Saskatchewan River Basin (NSRB). The tributaries of the Saskatchewan River flow from the Rocky Mountains across a vast area of interior plains that represents the largest area of drylands in Canada. We present an analysis of past and future climate and hydrology. We compare pre-industrial paleohydrology to model simulations of future climate and river flow. Research on the extent to which anthropogenic climate change departs from natural variability informs an assessment of the resilience of water resource policy and infrastructure, which were designed to operate under historical climatic variability. Human-induced climate trends are superimposed on natural multi-decadal climate variability, which is more evident and impactful at regional scales. Our case study of climate change and water security in the NSRB begins with a discussion of the drivers of hydroclimatic variability in this region.

2.1.1 Natural Variability of the Regional Hydroclimatic

Future projections of regional changes in precipitation and water resources are constrained by an incomplete understanding and simulation of the climate system, by making assumptions about anthropogenic forcing, and by a significant component of stochastic internal variability (Hawkins and Sutton 2009; Deser et al. 2012). Natural variability can dampen, mask or enhance human-induced trends with a larger influence at regional scales and for variables related to the water cycle. Barrow and Sauchyn (2019) found that in western Canada natural variability is the dominant source of uncertainty for the projection of future precipitation, accounting for more uncertainty than discrepancies among climate models and choice of greenhouse emission scenarios. These findings indicate that any attempts to project the climate of future decades require an understanding of natural variability in the regional hydroclimate and how well numerical models simulate this internal variability of the climate system.

Canada's western interior has a typical mid-latitude continental climate with large seasonal and inter-annual variability. Water allocation, and the design of storage and conveyance structures, is based primarily on average seasonal water levels, but otherwise water resources are managed to prevent the adverse impacts of flooding and drought. While these hydrological extremes are difficult to predict, their probability is strongly linked to periodic fluctuations in sea surface temperatures (Bonsal et al. 2019). Strong teleconnections between the regional hydroclimate and Pacific basin atmosphere–ocean oscillations drive much of the hydroclimatic variability at annual to decadal time scales, in some cases obscuring signals of climate change (Fye et al. 2006; Moore et al. 2007). Indices that describe the dynamics of these large-scale climate systems include the Pacific Decadal Oscillation (PDO), the Pacific North American (PNA) pattern and the El Niño Southern Oscillation (ENSO). The extreme phases of ENSO are inversely related to precipitation during the cold season: El Niño (La Niña) is associated with below (above) average precipitation in our region. There

is a strong negative relationship between the PDO and streamflow in western Canada; thus, water levels are higher when the PDO is in its negative phase and drier when the PDO is positive (St. Jacques et al. 2010). Gurrapu et al. (2016) demonstrated the strong influence of the PDO on peak river flows in western Canada. They found two distinct flood frequency curves for the negative and positive phases of the PDO. The curves diverge at higher return periods, indicating that flood flows are much more likely during the negative (cool) phase of the PDO.

Recent flooding and drought in the Prairie Provinces have been some of the most costly natural disasters in Canadian history. Studies of the drought in 2015 (Szeto et al. 2016) and floods in 2013 and 2014 (Teufel et al. 2017; Pomeroy et al. 2015) concluded that these naturally occurring events were intensified by human-caused climate change. One of the most robust climate projections, globally (IPCC 2014), nationally (Zhang et al. 2019) and regionally (Gizaw and Gan 2015), is an increase in rainfall intensity. This excess water will occur as the warmer climate converges with the wet phase of the PDO and ENSO. Similarly, the dry phase also will be amplified, when there is an absence of rain but also higher temperatures than in the past (Tam et al. 2018). Climate model projections suggest increasing exposure of the Prairies to drought, especially in summer and fall (Bonsal et al. 2019). The worst-case scenario for the Prairie Provinces is the reoccurrence of consecutive years of severe drought, such as occurred in the 1930s and in preceding centuries (Sauchyn et al. 2015). The warmer climate will amplify the impacts of a future prolonged drought. Meteorological drought (lack of rain) immediately affects dryland farming, while hydrological drought (low water levels) impacts irrigation, municipal and industrial water supplies.

2.2 Climate and Hydrology of the Upper North Saskatchewan River Basin

The North Saskatchewan River Basin (NSRB) is a headwater sub-basin of the larger Nelson River Basin, extending from the Rocky Mountains to Hudson Bay. Above Edmonton, Alberta, the NSRB has a drainage area of 28,100 km² and elevations that range between 611 and 3543 m above sea level (Fig. 2.1). The North Saskatchewan River (NSR) begins at the toe of the Saskatchewan Glacier in the Columbia Icefields, which have experienced dramatic changes, losing 22.5% of their total area between 1919 and 2009 (Tennant and Menounos 2013). The Saskatchewan Glacier and perpetual snows in the Rocky Mountain maintain river flow through the late spring and summer months. Land cover in the NSRB ranges from the alpine and montane ecosystems of the Rocky Mountains, to foothills forest, and the grassland, aspen parkland and agricultural landscape of the northern Great Plains. Even though the plains landscape comprises about 60 per cent of the drainage area, it yields a small proportion of the annual runoff given the sub-humid climate.

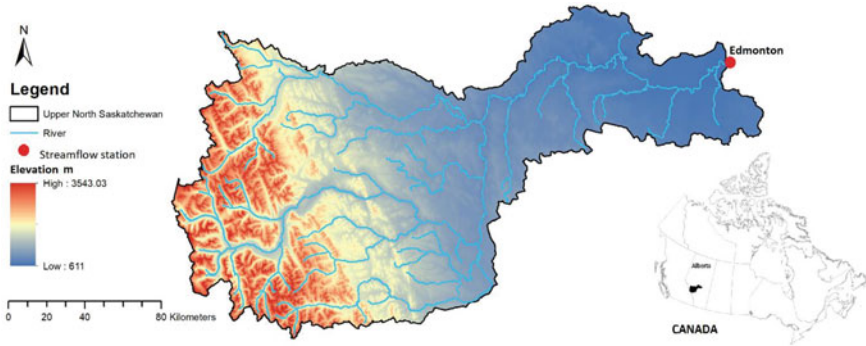


Fig. 2.1 Location, river network and elevations of the drainage basin of the North Saskatchewan River above Edmonton, Alberta

2.2.1 Climate

Environment and Climate Change Canada (ECCC) and its predecessors have monitored water and weather across a national network of gauges since the 1880s. Historical water and weather data are readily available from the websites of the Water Survey of Canada (<https://wateroffice.ec.gc.ca>) and the Meteorological Service of Canada (https://climate.weather.gc.ca/historical_data/), respectively. These monitoring networks were first installed in western Canada to locate reliable sources of water for irrigation, transportation and crop production. Thus, the location of the gauges on local streams, and of weather stations at agricultural research stations and airports, was initially the most important consideration when establishing these networks. Fortunately, the continuity of some of these hydrometric and meteorological stations has been maintained, because long records are vital for understanding the variability and change in our hydroclimate.

ECCC's database of Adjusted and Homogenized Canadian Climate Data (<https://ec.gc.ca/dccha-ahccd/>) (AHCCD) was created for use in climate research including climate change studies (Vincent et al. 2012; AHCCD 2017). It incorporates a number of adjustments applied to the original weather station data to address shifts due to changes in instruments and in observing procedures (Vincent et al. 2012; AHCCD 2017). During the period 1979–2016, the average minimum temperature for the NSRB was -12.3 °C and the average maximum temperature was 13.6 °C. Total annual precipitation averages 620 mm. The Rocky Mountain ranges of western Canada block much of the moisture brought by westerly winds from the Pacific. As a result, the annual precipitation is as high as 2000 mm at high elevations and as low as 300 mm in the plains (Environment Canada 1995).

Figure 2.2 is a time series of the mean annual temperature recorded at Edmonton since 1880. The annual average temperatures have ranged between -1 and 5 °C. Not only are there large differences in temperature between years, but there are also consecutive years of warmer (e.g. mid 80s to early 90s) and cooler (e.g. mid 60s to

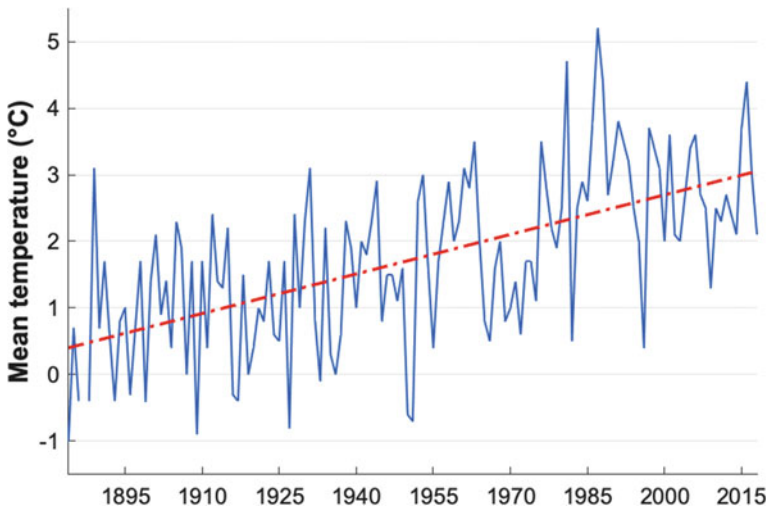


Fig. 2.2 Mean annual temperature at Edmonton since 1884 and the linear upward trend in red

mid 70s) weather. This variability from year-to-year and decade-to-decade tends to obscure a statistically significant upward trend. Nevertheless, the region is getting warmer; mean annual temperature has risen by more than 2 °C. Similar results were found by Jiang et al. (2017), when they analysed the seasonal trends in precipitation and temperature across Alberta using the Canadian Gridded Temperature and Precipitation Anomalies (CANGRD) dataset and found a consistent regional pattern of increasing temperature over all seasons.

While Fig. 2.2 illustrates a statistically significant ($p < 0.001$) rise of 2.7 °C in mean annual temperature, these data averaged for the whole year hide an important fact; most of the warming is occurring in winter to the lowest temperatures. Thus, western Canada is not getting hotter; it is getting much less cold. Figure 2.3 is a plot of mean daily minimum winter (DJF) temperature at Edmonton from 1884 to 2018. The statistically significant ($p < 0.001$) increase is 6.5 °C. There is large natural variability around this upward trend. The warmest winter was in 1931 during a very strong El Niño. Over the past three decades, the two coldest winters had a mean daily minimum temperature of approximately -20 °C. These would have been average winters for most of the twentieth century.

Total annual precipitation at Edmonton since 1884 is plotted in Fig. 2.4. It ranges from 250 to 800 mm from dry to wet years. The red dashed line indicates a linear upward trend; however, the increase is small relative to the range of values and large inter-annual and decadal variability. Even though most of the precipitation occurs in spring and early summer, winter precipitation (mostly snow) is more effective in producing soil moisture and runoff, since much of the summer rainfall is lost by evapotranspiration.

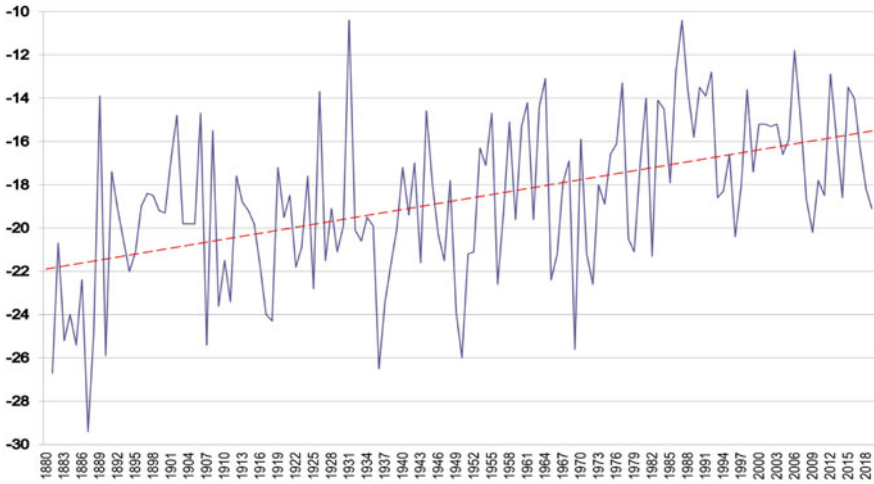


Fig. 2.3 Mean daily minimum winter (DJF) temperature (°C) at Edmonton, 1884–2019

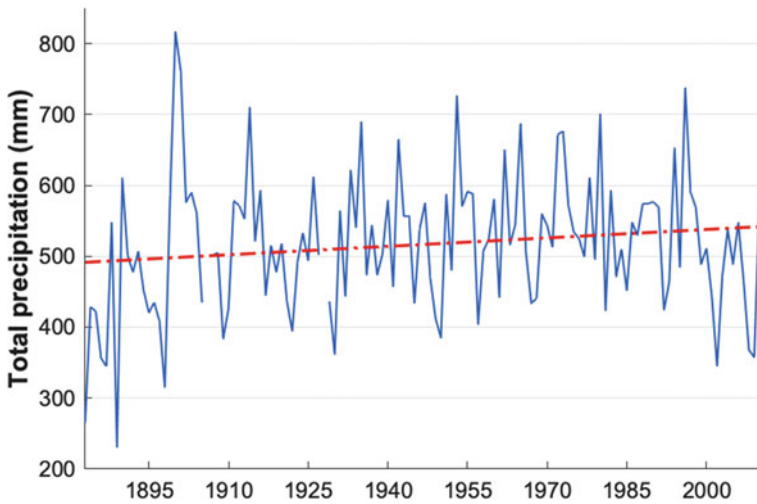


Fig. 2.4 Total annual precipitation at Edmonton since 1884, with an upward trend in red

2.2.2 Hydrology

The climate of the mountainous region of the NSRB (Fig. 2.1) is characterized by high precipitation and low evapotranspiration, resulting in high water yield. The mean annual discharge of the NSR at Edmonton is 215 m³/s. In Alberta, the NSRB drains an area of about 57,000 km² (Fig. 2.5; NSWA 2014). It is sub-divided into



Fig. 2.5 Sub-basins of the North Saskatchewan River Basin (NSWA 2012)

12 sub-basins. The Cline, Brazeau, Ram and Clearwater rivers, which are headwater tributaries in the Rocky Mountains, generate 88% of the total annual runoff (NSWA 2012).

2.2.2.1 Historical Streamflow Records

The streamflow gauge at Edmonton (05DF001) was recording natural flows of the North Saskatchewan River from 1911 until the mid 1960s when the Brazeau and Bighorn dams were built. Water is released from these reservoirs throughout the year for power generation, and there is little capacity to control or mitigate flooding of the NSR (EPCOR 2017). The River Forecast Centre of Alberta Environment and Parks has reconstructed naturalized flows by computing unregulated flows at the reservoir sites and routing these flows to Edmonton. While operation of the dams has little overall effect on mean annual flows, it increases flows in the cold season (Oct–Apr) and decreases them in the warm season (May–Sep). This is illustrated in Fig. 2.6, which is plot of mean monthly flow of the NSR at Edmonton from 1912–1971 prior to the Bighorn Dam, and from 1972–2015, after the construction of the Dam. The natural flow (the blue bars) is characteristic of mid-latitude mountain watersheds with a snow-dominated hydrologic regime, where approximately 40% of the annual discharge occurs in June and July from rainfall and melt of the mountain snowpack.

Figure 2.6 shows that relatively high flows are maintained throughout the summer from the melt of snow and glaciers at high elevations. MacDonald et al. (2012)

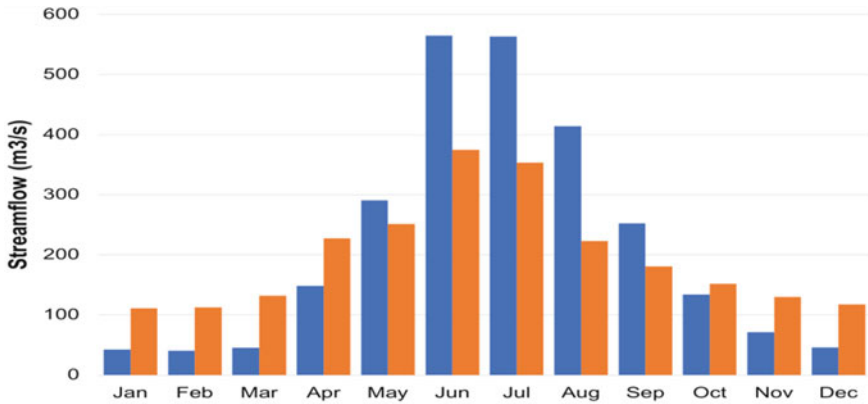


Fig. 2.6 Mean monthly flow (m^3/s) of the North Saskatchewan River (NSR) at Edmonton from 1912–1971 (blue) and 1972–2015 (orange), before and after construction of the Bighorn Dam

modelled the future snowpack of the NSRB, quantifying potential changes in snow water equivalent. They found that there may be little change in the annual maximum snow accumulation; however, spring snow melt likely will occur earlier as the climate warms and with an increase in the proportion of rain versus snow. The accelerated retreat of mountain glaciers in recent decades is an indication of repeated years of negative mass balance, where melt of glacier ice in summer exceeds the contribution of new ice converted from the winter snowpack. Among the five major rivers that flow from the eastern slopes of the Rocky Mountains, the North Saskatchewan is fed by the largest ice volume and area of glaciers (about 1% of the watershed above Edmonton; Marshall et al. 2011). Recent trends and modelling of glacier mass balance suggest that glaciers on the eastern slopes of the Rockies will lose 80–90% of their volume by 2100, with a corresponding decline in glacier contributions to streamflow (Marshall et al. 2011). The contribution of glacier meltwater to the NSR is less than 3% of the regulated flow at Edmonton during July through September (Comeau et al. 2009). While the loss of glacier ice has generated extra runoff from the larger glaciers, the number of glaciers is declining as the smaller ice masses disappear. Figure 2.7, a time series of annual flow of the NSR at Edmonton, shows a downward trend, but also considerable interannual and decadal variability reflecting the influence ENSO and the PDO on the regional hydroclimate (St. Jacques et al. 2010, 2014; Gurrupu et al. 2016; Sauchyn et al. 2011, 2015). It should be noted that this gauge station is located downstream of two water treatment plant intakes and does not account for the portion of withdrawals that are returned to the NSR (EPCOR 2017).

In Fig. 2.8, naturalized streamflow from 1912–2010 is plotted for each season: winter (DJF), spring (MAM), summer (JJA) and fall (SON). The linear trends (red lines) are not statistically significant in spring and fall; however, they are significant ($p < 0.05$) in winter and summer, with an increase of $8.5 \text{ m}^3/\text{s}$ and a decrease of $113.7 \text{ m}^3/\text{s}$, respectively. These streamflow trends are consistent with climate changes over the past century. Warming has led to winter snowmelt, and less snow and ice

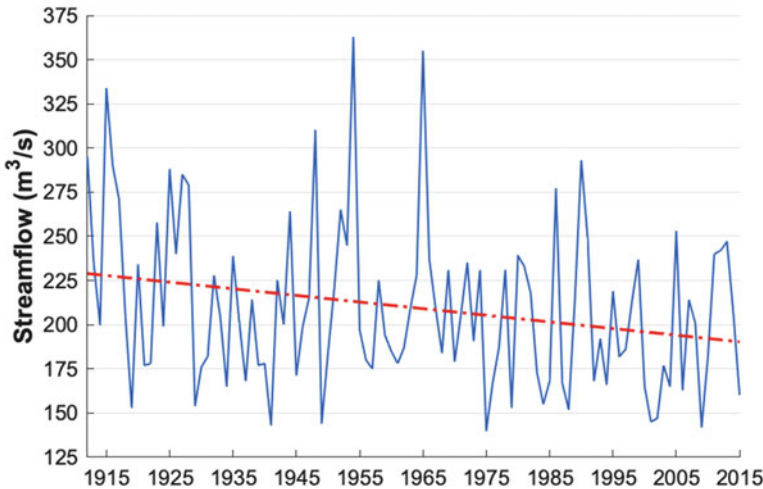


Fig. 2.7 Mean annual flow (m^3/s) of the North Saskatchewan River (NSR) at Edmonton, 1912–2015. The red line represents a downward linear trend

remain at high headwater elevations to sustain summer flow. These flow series are also marked by large differences between years and decades, such that short-term trends can reflect natural variability rather than climate change.

In Fig. 2.9, water-year hydrographs are plotted for three time periods. This comparison of observed natural flows of the North Saskatchewan River at Edmonton shows a decrease in spring/summer flows in the past 30 years and an increase in winter flows. This is consistent with the trends in the time series of annual flows by season (Fig. 2.8), which show an upward trend in winter and a downward trend in summer flows. The total annual flows increased 3.5% for the period of 1950–1979 and decreased 5.3% for the period of 1980–2010 compared to the base period of 1912–1941.

Detection and attribution of climate cycles is necessary to distinguish natural climate variability from trends imposed by global climate change. The wavelet transformation of climate time series assigns power to the spectrum of frequencies across the time domain. Figure 2.10 is a continuous wavelet plot for natural NSR flow at Edmonton from 1912–2010. The power at low frequencies corresponds to the decadal variability of the PDO and, at two to four years, the continuous effect of ENSO.

2.2.2.2 Groundwater

Further growth in Alberta's population and economy could place increasing demands on groundwater systems (Grasby et al. 2009; Worley Parsons 2009; Hughes et al. 2017). The Paskapoo Formation in west-central Alberta is an important aquifer and source of groundwater for industrial use, primarily in the oil and gas industry (Hughes et al. 2017). Data on groundwater levels is available from the Alberta Groundwater

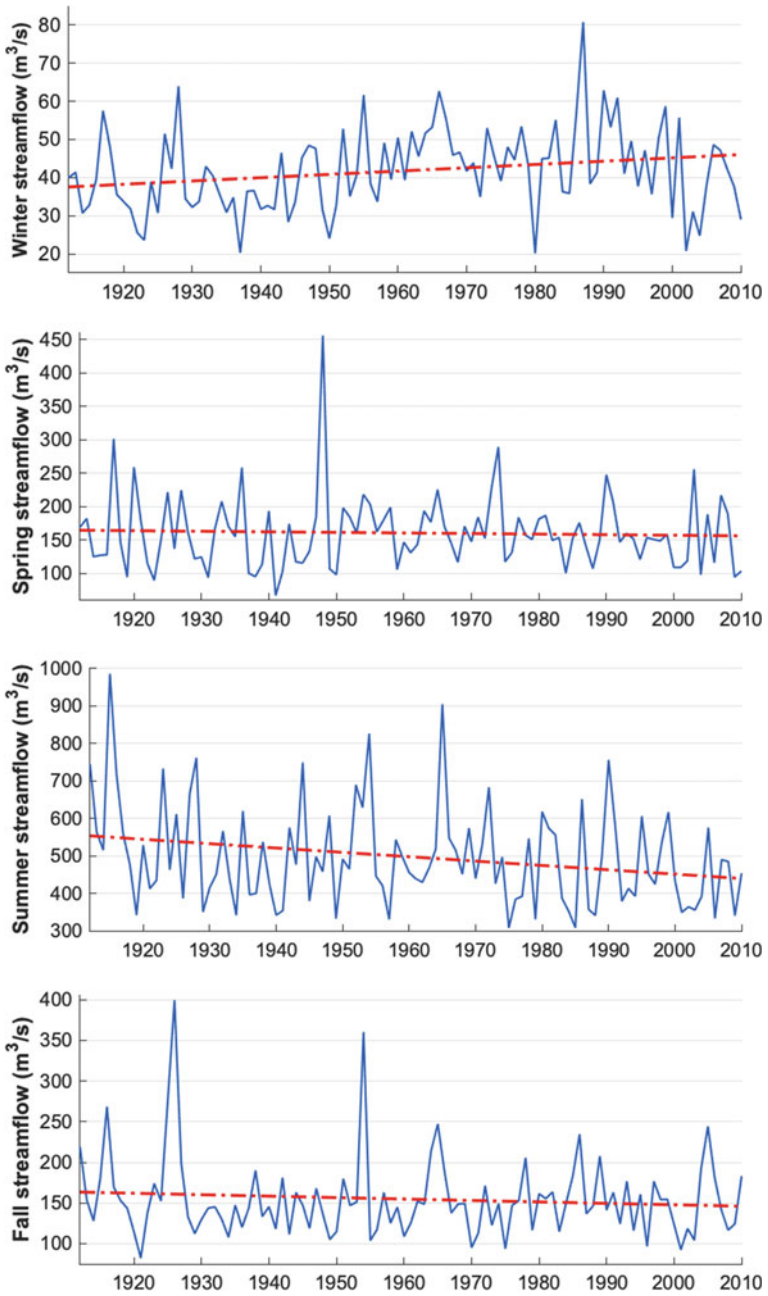


Fig. 2.8 Naturalized flow (m³/s) of the North Saskatchewan River (NSR) from 1912 to 2010 at Edmonton by season

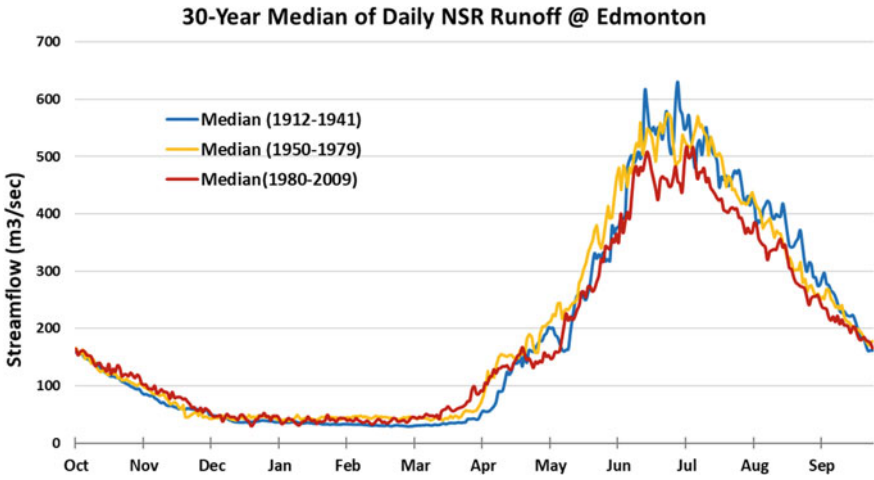


Fig. 2.9 Comparison of median of 30-year daily natural streamflow for North Saskatchewan River at Edmonton for three different time periods

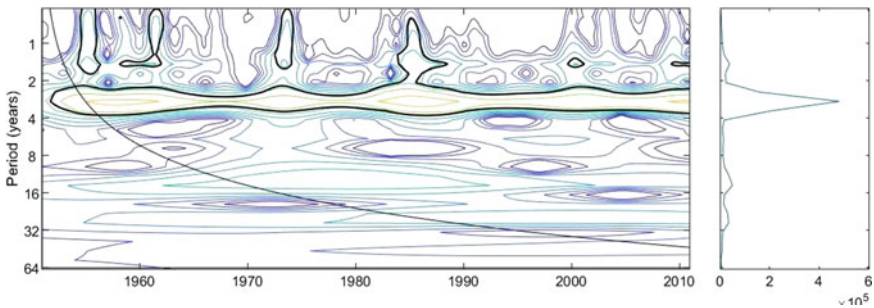


Fig. 2.10 Continuous wavelet plot for NSR natural streamflow at Edmonton from 1911–2010

Observation Well Network (<https://aep.alberta.ca/water/programs-and-services/groundwater/groundwater-observation-well-network/>). Data from these observation wells demonstrates the influence of climatic variability on groundwater table elevation, but as yet there is no evidence of the impact of a warming climate on groundwater recharge (Perez-Valdivia and Sauchyn 2012). Research has shown that when ENSO and PDO are in their respective positive phases, groundwater levels reflect the resulting warmer and drier winters and reduced groundwater recharge (Hayashi and Farrow 2014; Perez-Valdivia and Sauchyn 2012).

2.2.3 *The Paleohydrology of the NSRB*

Understanding the long-term natural variability of the regional hydroclimate is an important precursor to research on the impacts of climate change. Natural proxy records of hydroclimate, such as tree-ring chronologies, provide knowledge of past climate-driven non-stationarities in hydrologic variables. Ring-width data from long-lived trees growing at dry sites are a proxy of seasonal and annual water levels. The growth of these trees is limited by the availability of soil moisture, and the same weather variables (precipitation, temperature, evapotranspiration) that determine river flow also control tree growth. As a result, there is a similar integrating and lagged response of tree growth and streamflow to inputs of precipitation (Kerr et al. In review; Sauchyn and Ilich 2017).

We reconstructed estimates of warm (May–September) and cool (October–April) season streamflow for the NSR at Edmonton from multi-species measurements of annual ring width (RW), earlywood width (EW) and latewood width (LW) using standard methods in dendrohydrology (Meko et al. 2012). Multiple linear regression (MLR) using a forward stepwise procedure with a cross-validation stopping rule (leave n-out) was used to model and reconstruct warm and cool season streamflow from 1200 to 2015. The tree-ring models were calibrated over the full instrumental naturalized streamflow record (1912–2010) using a nested approach, where shorter tree-ring chronologies are dropped from the pool of predictors and the procedure is repeated using the remaining longer series. No more than five chronologies were used for each reconstruction nest, in order to avoid multi-collinearity and an over-fit model, while achieving maximum reduction of the residual variance not accounted for by predictors already in the model. Predictors included lagged (\pm two years) chronologies to account for any differences in the timing of the response of streamflow and tree growth to inputs of precipitation and snow meltwater.

Following the methods of Kerr et al. (In review), each nest of estimated streamflow is a discrete independent reconstruction (i.e. for each season), using tree-ring chronologies that positively correlate with either warm or cool season streamflow, or both. None of the same chronologies was used as potential predictors in the other reconstruction. This procedure was applied to minimize inter-seasonal correlation in the tree-ring reconstructed estimates of streamflow, which can be seen in sub-annual chronologies (i.e. EW and LW) from the same tree (Stahle et al. 2020; Kerr et al. In review). Calibration and verification statistics indicate skilful reconstructions of warm and cool season streamflow from robust models with considerable predictive power. The models accounted for up to 65% of the naturalized streamflow instrumental variance. As illustrated in Fig. 2.11, the reconstructions replicated the inter-annual variability in historical streamflow, but are better at capturing low flows, while underestimating high flows, throughout the calibration period. Underestimation of peak flows is a common limitation of dendrohydrology, as there is a biological limit to the response of tree growth to high precipitation and low evapotranspiration during wet years. Nested models were discarded after approximately

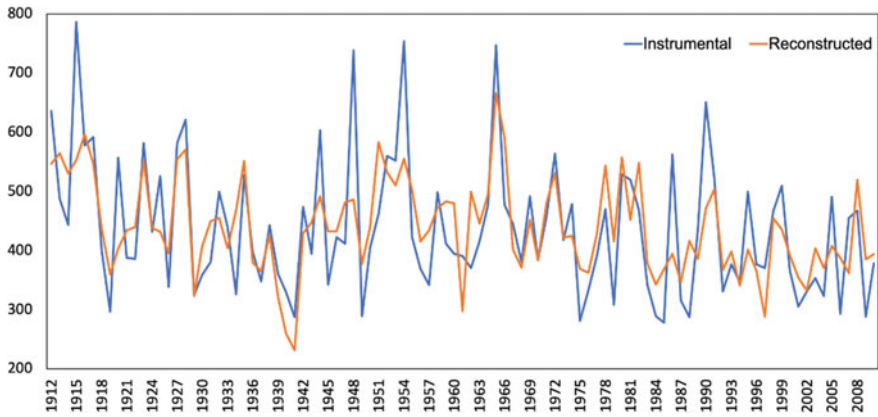


Fig. 2.11 NSR at Edmonton instrumental and tree-ring reconstructed warm season streamflow (m^3/s) for the calibration period, 1912–2010

1200, as R^2_{adj} values began to decline to below 35%, and other descriptive statistics indicated the model prediction was declining, due to a lack of sample depth of statistically significant chronologies.

In Figs. 2.12 and 2.13, the reconstructions (1200–2015) of the warm and cool seasonal flow of the NSR at Edmonton are shown as anomalies (departure from the mean). The seasonal paleohydrology reflects the natural variability of the climate recorded in the tree-rings. The low flow years of the instrumental record (i.e. 1930s,

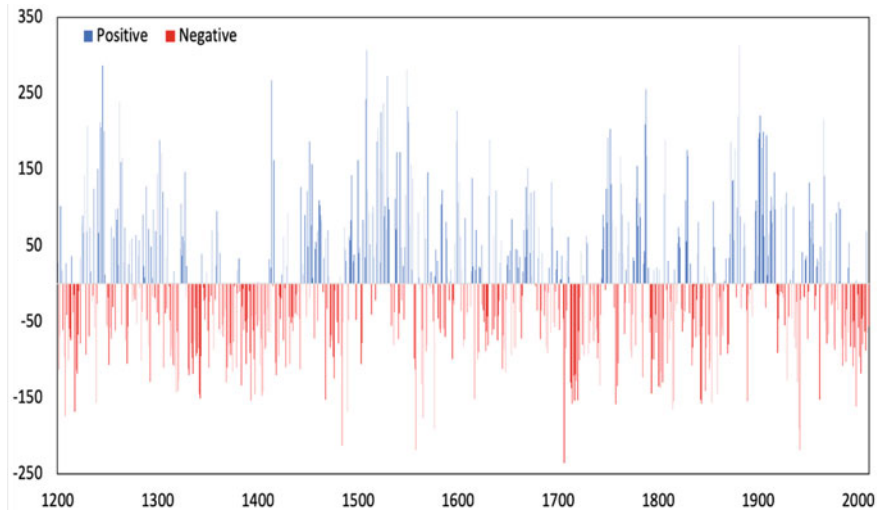


Fig. 2.12 Tree-ring reconstructed warm season (May through August) streamflow (m^3/s) plotted as positive (blue) and negative (red) departures from the mean warm season flow for the NSR at Edmonton, 1200–2015

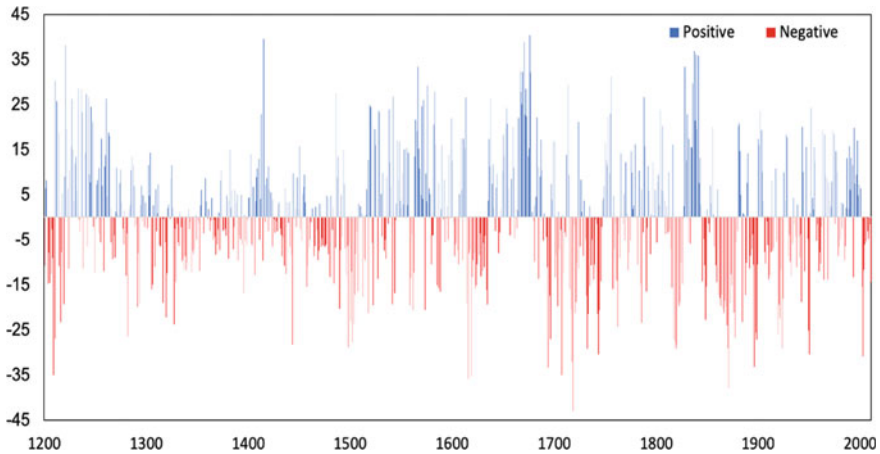


Fig. 2.13 Tree-ring reconstructed cool season (December through April) streamflow (m^3/s) plotted as positive (blue) and negative (red) departures from the mean cool season flow for the NSR at Edmonton, 1200–2015

1980s and early 2000s) are clearly visible. Even more noticeable are periods of low flow that exceed the historical worst-case scenario in terms of severity and duration (i.e. fourteenth and fifteenth centuries in the warm season record). Decadal scale variability is also evident in these plots, in terms of successive years of high and low flows, which last one to three decades. In both seasons, low- and high-water levels reoccur at more or less regular intervals.

We further explored the reconstructed time series of warm and cool season streamflow for a better understanding of the global drivers of the natural variability in the regional hydroclimate. The long-term seasonal impacts of slowly varying modes of sea surface temperature (SST) variability are realized in their decadal-to-multidecadal effects on other teleconnections and large-scale atmospheric circulation (Howard et al. 2019). We identified the main oscillatory modes of variability in the NSRB paleohydrology using continuous wavelet transform (Grinsted et al. 2004) of the reconstructed warm and cool seasonal flows of the NSR at Edmonton. The wavelet plots in Figs. 2.14 and 2.15 show significant multi-decadal and inter-annual modes of variability, which can be linked to the influence of the PDO and ENSO on the hydroclimate of western North America (St. Jacques et al. 2010; Sauchyn et al. 2015; Gurrupu et al. 2016; Sauchyn and Ilich 2017).

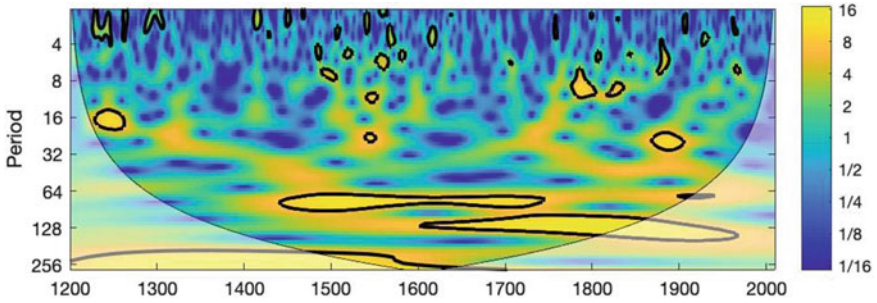


Fig. 2.14 Continuous wavelet power spectrum for warm season tree-ring reconstructed streamflow (1200–2015) of the NSR at Edmonton. Thick black contour lines indicate significance at 95% level

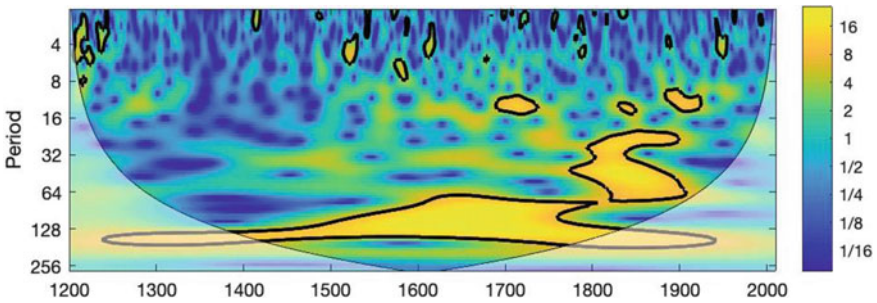


Fig. 2.15 Continuous wavelet power spectrum for cool season tree-ring reconstructed streamflow (1200–2015) of the NSR at Edmonton. Thick black contour lines indicate significance at 95% level

2.3 Water Use and Demand

2.3.1 Historical Water Use

The security of water supplies is function of not only supply, but also the demands placed on these supplies for industrial and residential use. Information on the use and consumption of water in the Edmonton region is available from the annual reports compiled by EPCOR Water Canada and from studies for the North Saskatchewan Watershed Alliance (NWSA) by AMEC (2007) and Thompson (2016). Additional province-wide data from the Alberta Water Use Reporting System (<https://aep.alberta.ca/water/reports-data/water-use-reporting-system/default.aspx>) indicate that 70% of licenced surface water use in the NSRB occurs within the Capital Region (Strawberry, Sturgeon, Beaverhill sub-basins; Fig. 2.5). This region had a slight increase in water allocations and use in 2016 compared to 2006, with a large increase in commercial water use and decrease in industrial water use. About 20% of the licenced surface water use occurs within the Headwaters Region (Cline, Brazeau, Ram, Clearwater, Modeste sub-basins). Water allocations and use within

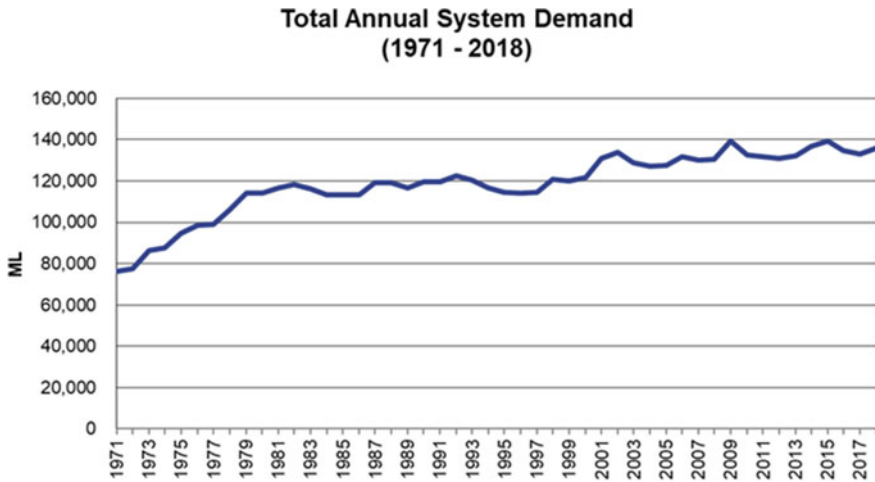


Fig. 2.16 Total annual demand, from 1971 to 2018, for the Edmonton regional water system. Source EPCOR Water Canada

the basin had changed slightly by 2016 compared to 2006: 2% increase for licenced withdrawals and 7% increase for licenced use (Thompson 2016).

Unlike the closed sub-basins (Bow, Oldman and SSR) in southern Alberta, Alberta Environment and Parks continues to grant water licences in the NSRB. About 20% of the NSR is allocated, while much less water is extracted. That is, full allocations are not being used and much of the water that is extracted is returned to the NSR. The amount of water in the NSR is large relative to the volume of water withdrawn by the Water Treatment Plants (WTPs) for drinking water purposes, which is less than 3% of the total daily flow (EPCOR 2017). Figure 2.16 is a plot of the total annual demand, from 1971–2018, for the Edmonton regional water system. There are two notable inflections in this demand curve. Demand rose through the 1970s and then levelled off until 2000 when there was another rise in demand to a slightly higher level. The mean average daily demand for 2001–2018 was 363 ML/d, and mean peak hour demand was 741 ML/d.

Figure 2.17 of average daily demand from 1971–2018 makes a distinction between the City of Edmonton, which accounts for most of the demand, and the larger metropolitan region. Regional water use has increased at a faster rate than in the city; it was almost 5 times higher in 2018 than in 1971, while in-city water use was only 1.5 times higher. By 2018, raw water intake increased by 24% compared to 1983. Data for in-city commercial total water consumption are available for 1991–2018 only; consumption decreased by 31% over this period.

While total consumption (residential, multi-residential, commercial and regional) in 2018 was 78% higher than in 1971, per capita Edmonton water consumption decreased. Total per capita water use in 2018 was 42% lower than the 1971–1980 average (31% lower than 2001), at 289 L/capita/d, while the city’s population increased by 2.1 times, from 462,572 (1971–1980 average) to 951,000 (2018).

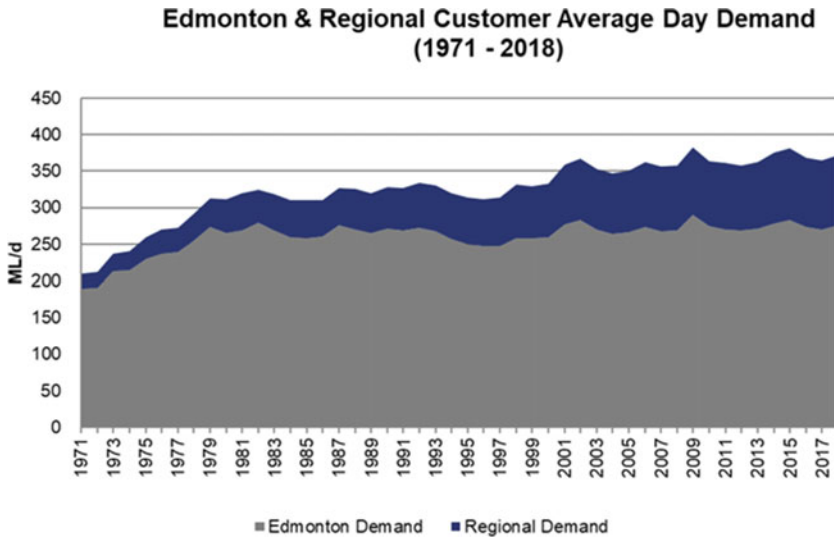


Fig. 2.17 Average daily water demand from 1971 to 2018 for the City of Edmonton and the larger metropolitan region. *Source* EPCOR Water Canada

Figure 2.18 clearly illustrates the decoupling of water demand from population growth. Since about 1980, per capita demand has declined at a significant rate while the population approximately doubled. Programmes and practices for the conservation and more efficient use of water have obviously been effective. Outdoor water use

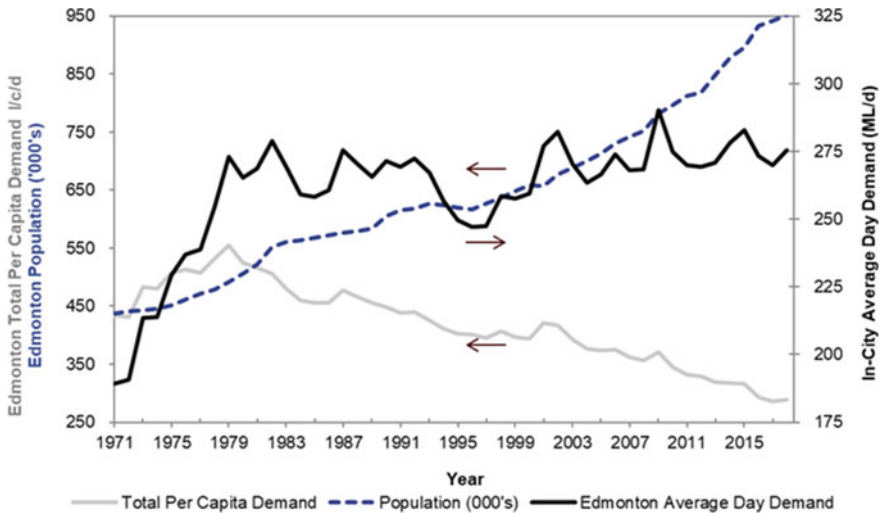


Fig. 2.18 Average daily demand, population and total per capita demand per year for the City of Edmonton from 1971 to 2018. *Source* EPCOR Water Canada

typically accounts for much of the water demand in North American cities. Although Edmonton has a relatively short summer compared to other cities, climate change projections of shorter winters and longer warmer summers could increase the demand for outdoor water use.

2.3.2 Projected Water Demand

Demand for water will grow in coming decades because Alberta's population is expected to reach 6.4 million by 2046, an increase of about 2.1 million people from 2017. It also is becoming more concentrated in urban centres; by 2046, almost 8 in 10 Albertans are expected to reside in the Edmonton–Calgary corridor (Treasury Board and Finance 2018). Based on population growth alone, increased demand for water is anticipated; however, water use and demand depend on other factors, including policies, population, infrastructure, technology, human behaviour and climate. While future water demand has been forecasted for Alberta River Basins, these studies considered different combinations of the determinants of demand, and some studies are outdated, for example, the forecasting of demand by 2015 (City of Calgary 2007).

AMEC Earth & Environmental (2007) completed an overview of current and future water use in Alberta for the Ministry of Environment. They examined licenced and actual water use to October 2006 for six sectors: municipal and residential, agricultural, commercial, petroleum, industrial and other. Forecasting was based on expected changes in population and economic activity. Thus, they were “business-as-usual” predictions since they did not account for improvements in water use efficiency. A 21% increase from current water use (2005) was the net result for the entire province; however, most of this increase was attributed to rising water demand in the irrigation and industrial (petroleum) sectors, and thus concentrated in the southern and more northerly river basins, respectively. For the NSRB, projections of the increase in water demand over 20 years (2005–2025) ranged from 15% for a low growth scenario to 118% for a high growth scenario. The increase in demand for a medium growth scenario was about 34%.

Accurate prediction of water usage is important for both short-term (operational) and long-term (planning) aspects of urban water management. Water demand forecasting models tend to overestimate long-term demands because they generally do not account for water conservation practices and reductions in per capita usage, such as the declining water consumption per customer over the past three decades at Edmonton (Fig. 2.18). As populations and economies grow, water demand does not necessarily increase at a proportional rate, given effective conservation and efficiency practices. A major “Residential End Uses of Water Study” (DeOreo et al. 2016) of North American water utilities found a 22% decrease in average annual indoor household water use from 1999–2016. Edmonton was one of three Canadian cities included in the study.

To improve the accuracy of demand forecasts for municipal water management, Liu and Davies (2019) developed a model for Edmonton and applied it to long-term

water demand forecasting using climate model projections of daily temperature and precipitation. Their model provides a projection of total demand based on inputs of daily and weekly water demand and meteorological variables. Their data-driven forecasting model is run in the framework of a system dynamics model that can be used to replicate physical structures and processes and explore the future demand for various water end uses under different scenarios related to policy, climate and population changes. The daily and weekly water demand models for Edmonton constructed by Liu and Davies (2019) reveal that maximum and average temperatures produce more accurate results than minimum temperature, probably because outdoor watering in summer relates more strongly to daytime average and high temperatures than to the daytime low. Furthermore, models using indices of the timing of water demand (e.g. “day-in-week” and “day-in-month”) produced significantly better results than those without these indices that capture the periodicity of water demand. Outdoor water demand in summer is an important component of municipal water demand.

2.4 The Future Climate of the NSRB

Projections of the future climate of the NSRB have been previously derived from output from Global Climate Models at a relatively coarse scale (100 s km) with down-scaling based on the statistical relationship between model and observed weather data (e.g. Jiang et al. 2017; Vaghefi et al. 2019). We have developed climate projections for the NSRB above Edmonton using high-resolution (25–50 km) data from Regional Climate Models (RCMs), which were applied to the dynamical down-scaling of Earth System Models (ESMs). We accessed output for an ensemble of 10 RCMs from the data repository of the North American domain of the Coordinated Regional Climate Downscaling Experiment (NA-CORDEX). All RCMs were forced with RCP 8.5, a high emissions pathway. Monthly, seasonal and annual mean temperature (°C) and total precipitation (mm) were computed by averaging values for model grid points within the boundary of the NSRB. We determined changes in 30-year average temperature and precipitation for the near (2021–2050) and mid (2051–2080) future compared to the climate of the baseline period 1981–2010. Table 2.1 gives the multi-model mean changes. Mean temperature and total precipitation are projected to increase on seasonal and annual scales, with the greatest changes during the cool period (fall, winter). Mean summer temperature is expected to increase by 3.5 °C with almost no change in total precipitation.

Whereas Table 2.1 presents the mean multi-model climate changes, the scatterplot in Fig. 2.19 shows the range of mid-future (2051–2080) projections derived from the 10 RCMs. Increases in annual precipitation and temperature range from 2 to 18% and 2 to 4.5 °C, respectively. The largest temperature changes highlighted in Table 2.1 occur in winter. Figure 2.20 presents evidence of a dramatic decline in the frequency of extreme winter temperatures at Edmonton, as simulated by the Canadian Regional Climate Model version 5, with boundary conditions from the Community Earth System Model version 2 (CRCM5_cesm2). Since this is a model simulation,

Table 2.1 Multi-model mean changes in temperature and precipitation for near (2021–2050) and far (2051–2080) future compared to baseline (1981–2010)

Period	Climatic variable	2021–2050	2051–2080
Annual	Mean temperature (°C)	1.9	3.7
	Maximum temperature (°C)	1.7	3.4
	Minimum temperature (°C)	2.1	4.0
	Total precipitation (mm)	32.5	54.2
	Total precipitation (%)	6.9	11.5
Spring (MAM)	Mean temperature (°C)	1.8	3.0
	Maximum temperature (°C)	1.6	2.7
	Minimum temperature (°C)	2.1	3.3
	Total precipitation (mm)	9.5	26.9
	Total precipitation (%)	10.5	29.4
Summer (JJA)	Mean temperature (°C)	2.3	3.5
	Maximum temperature (°C)	2.4	3.6
	Minimum temperature (°C)	2.1	3.6
	Total precipitation (mm)	9.0	7.4
	Total precipitation (%)	3.9	3.3
Fall (SON)	Mean temperature (°C)	1.3	3.7
	Maximum temperature (°C)	1.1	3.5
	Minimum temperature (°C)	1.7	3.8
	Total precipitation (mm)	17.2	25.0

(continued)

Table 2.1 (continued)

Period	Climatic variable	2021–2050	2051–2080
Winter (DJF)	Total precipitation (%)	21.2	30.9
	Mean temperature (°C)	2.2	4.9
	Maximum temperature (°C)	1.9	4.1
	Minimum temperature (°C)	2.5	5.5
	Total precipitation (mm)	8.8	15.3
	Total precipitation (%)	13.9	24.0

The largest increases are highlighted with bold font

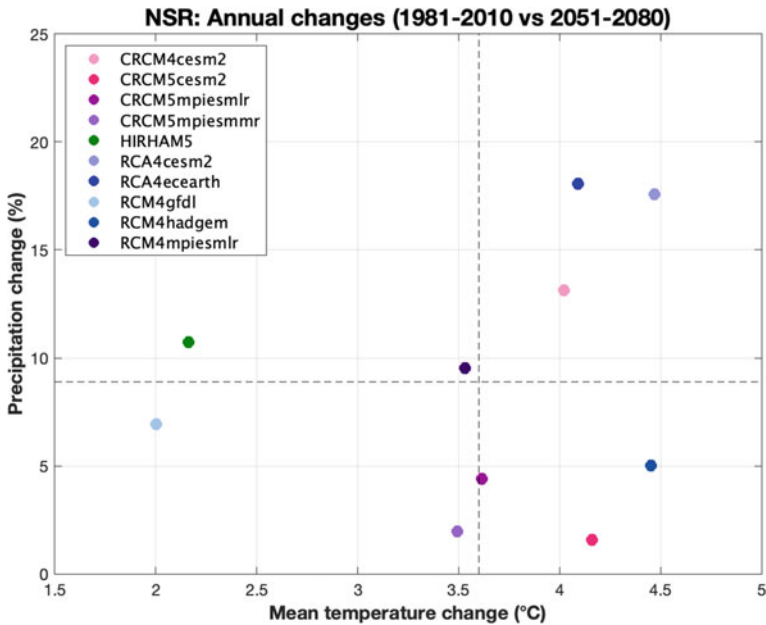


Fig. 2.19 Scatterplot of climate change projections derived from 10 RCMs

the sequence of extreme temperatures is arbitrary. A different RCM would produce a different sequence, although statistically (i.e. the range and trend) the results would be very similar.

Figures 2.21 and 2.22 are time series of total summer and spring precipitation, respectively, for the North Saskatchewan River Basin above Edmonton. For the

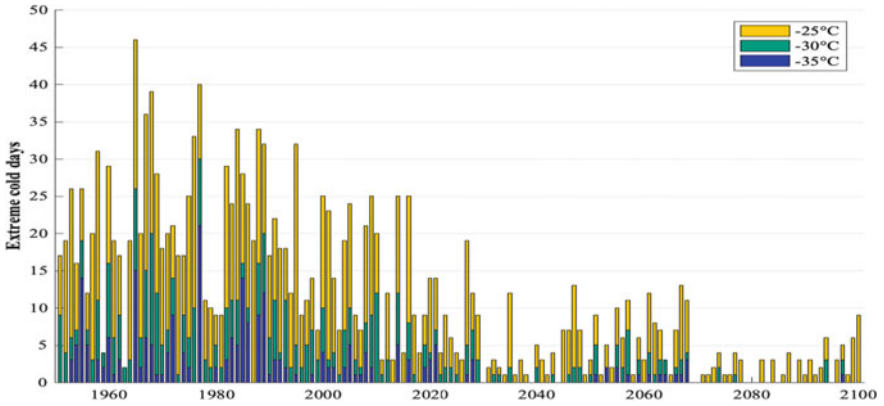


Fig. 2.20 Extreme minimum temperatures at Edmonton, 1951–2100, as simulated by CRCM5_cesm2 and RCP 8.5

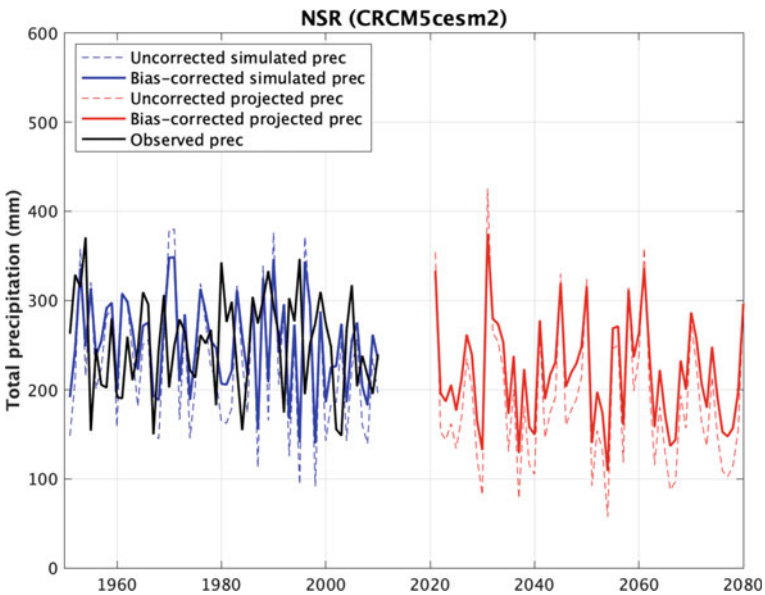


Fig. 2.21 Simulated and observed (1951–2015) total summer precipitation, North Saskatchewan River Basin above Edmonton. The bias corrected data is from CRCM5_cesm2

historical period (1951–2015), both simulated and observed data are shown. The historical and projected (2021–2080) model output is from CRCM5_cesm2 and was bias corrected. These plots illustrate a contrast between the negligible change in summer versus an upward trend in and spring. They also display the large inter-annual and decadal variability characteristic of the hydroclimate of the region.

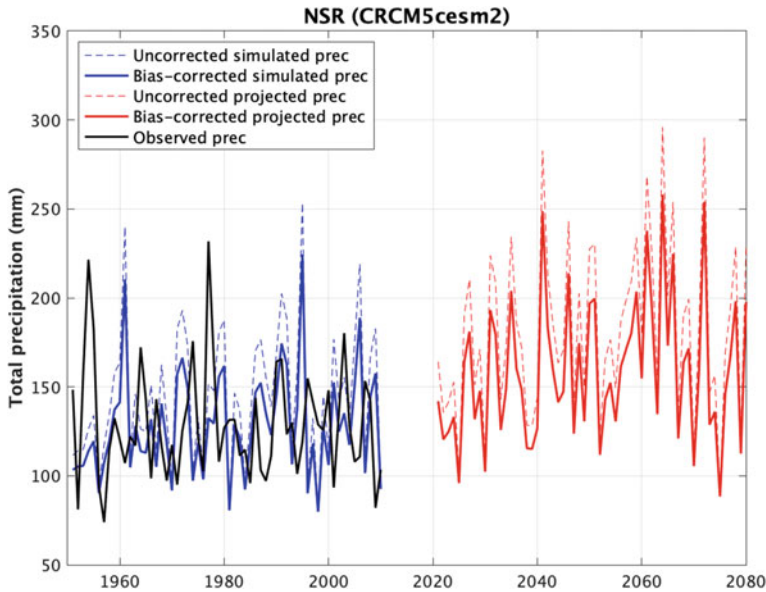


Fig. 2.22 Simulated and observed (1951–2015) total spring precipitation, North Saskatchewan River Basin above Edmonton. The bias corrected data is from CRCM5_cesm2

Figure 2.23 is a plot of the projected maximum daily precipitation changes at Edmonton from 1950 to 2100 as simulated by the CRCM5_cesm2 (RCP 8.5). According to the scatterplot in Fig. 2.16, this RCM/ESM experiment projects the least change in annual precipitation, plotting at about 2% on the vertical axis. Despite the negligible change in total annual precipitation, precipitation on one future day far exceeds prior extreme events. This time series also displays inter-annual and decadal variability; years with heavy precipitation events tend to cluster in wet decades and with dry decades in between.

2.5 Hydrological Response to Projected Climate Changes

Previous research on the impact of climate change on the North Saskatchewan River (NSR) (Golder 2008; Kienzle et al. 2012) found increased flow during winter and spring, earlier spring melt and decreased flow during the summer and fall. These shifts in the seasonal distribution of river flow are in response to projected climate changes: a warmer wetter winter and a warmer and possibly drier summer. Summer flows are impacted by reductions in the extent of glacier ice and summer snowpack at high elevations in the headwaters. These prior studies were based on the use of data from GCMs as inputs to hydrological models to project changes in average seasonal

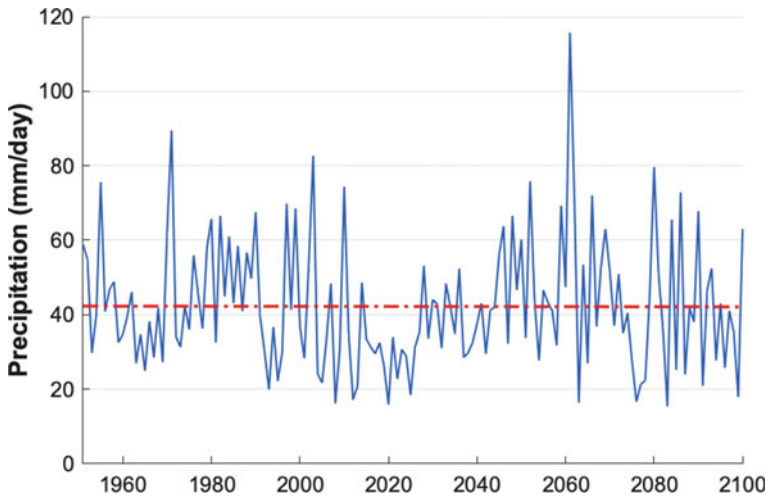


Fig. 2.23 Maximum daily precipitation at Edmonton, 1950–2100, as simulated by the CRCM5_cesm2 and RCP 8.5

flows. In contrast, our work is based on the use of high-resolution climate change projections from RCMs to drive runs of a calibrated distributed hydrological model.

2.5.1 Hydrological Modelling of the NSRB Above Edmonton

We simulated the hydrology of the NSRB above Edmonton using the Modélisation Environnementale–Surface et Hydrologie (MESH) grid-based modelling system (Fig. 2.24). MESH is a standalone land surface-hydrology model developed initially by Environment and Climate Change Canada (Pietroniro et al. 2007). It has been widely applied to various cold regions of Canada (Davison et al. 2006; Pietroniro et al. 2007). MESH has three components: (1) the Canadian Land Surface Scheme (CLASS) (Verseghy 1991; Verseghy et al. 1993) that computes the energy and water balances using physically based equations for soil, snow and vegetation canopy at a 30 min time step, (2) lateral movement of soil and surface water to the drainage system with either of the algorithms called WATROF (Soulis et al. 2000) or PDMROF (Mekonnen et al. 2014), and (3) hydrological routing using WATFLOOD (Kouwen et al. 1993) that collects overland flow and interflow from each grid cell at each time step and routes them through the drainage system. The river routing is based on a storage routing technique in which the channel roughness and storage characteristics control the inflows from the local grid and upstream river reach. The land model is run on each tile independently. The overall fluxes and prognostic variables for each grid cell are obtained by taking a weighted average of the results from tiles.

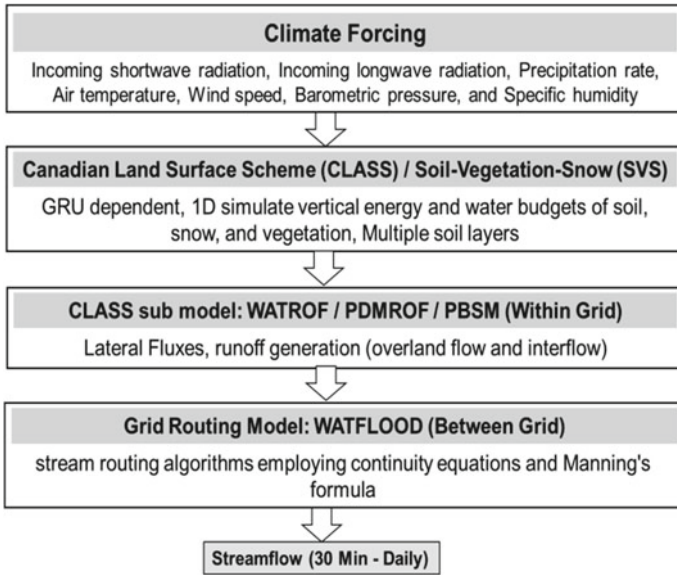


Fig. 2.24 MESH land-surface and hydrology modelling system schematic diagram

A 0.125° drainage database consisting of 278 grid cells was constructed using the Green Kenue tool (v3.4.3) as shown in Fig. 2.25. Topographic data was from the Canadian Digital Elevation Model (CDEM 2015) at a scale of 1:250,000. The shape files

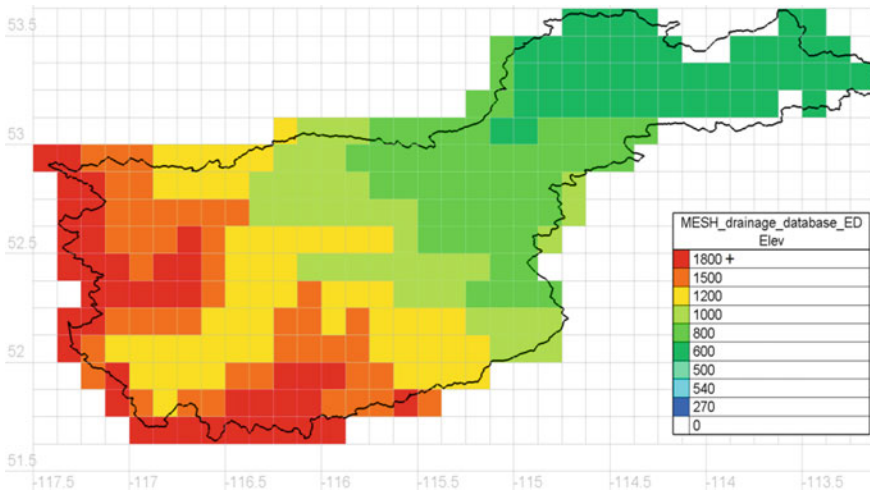


Fig. 2.25 Drainage database of NSR at Edmonton. Each grid represents one Grouped Response Unit (GRU) with soil, land use, drainage area, elevation, channel length and slope data

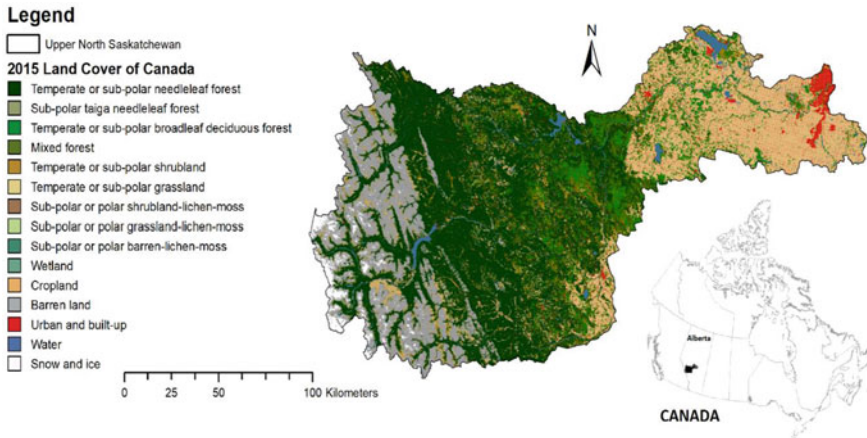


Fig. 2.26 Land-cover classification of Upper North Saskatchewan River Basin generated by the Canada Centre for Remote Sensing (CCRS)

of the catchment and rivers are available from the National Hydro Network—NHN—GeoBase Series (<https://open.canada.ca/data/>). The soil data was acquired from Agriculture and Agri-Food Canada. The 30-m land-cover data (Fig. 2.26, Pouliot et al. 2017) was obtained from the Canada Centre for Remote Sensing (CCRS). Twelve land-cover types were used to define Grouped Response Units (GRUs). For computational efficiency, a GRU-based approach combines areas of similar hydrological behaviour to address the complexity and heterogeneity of the drainage basin. Each model grid cell is represented by a limited number of distinct GRUs (tiles) weighted by their respective cell fractions. For large basins, this approach has been found more efficient with its operational simplicity while retaining the basic physics and behaviour of a distributed model (Pietroniro and Soulis 2003).

2.5.2 Calibration and Validation of the MESH Model

The MESH model was calibrated and validated using the bias-corrected historical gridded climate data WFDEI-GEM-CaPA (Asong et al. 2018). Future flows were simulated using bias-corrected data from 15 runs of the Canadian Regional Climate Model (CanRCM4) based on the RCP8.5 emission scenario (Asong et al. 2020; Scinocca et al. 2016). Running MESH requires three hourly climate forcing data for seven variables: shortwave radiation, longwave radiation, precipitation rate, air temperature, wind speed, barometric pressure and specific humidity.

Figure 2.27 is a plot of observed and simulated daily runoff of the NSR at Edmonton for the calibration (Feb 1995–Dec 2002) and validation (Jan 2003–Dec 2010) periods. Goodness of fit results for the calibration and validation are given in Table 2.2. The calibration NSE of 0.69 indicates good agreement between modelled

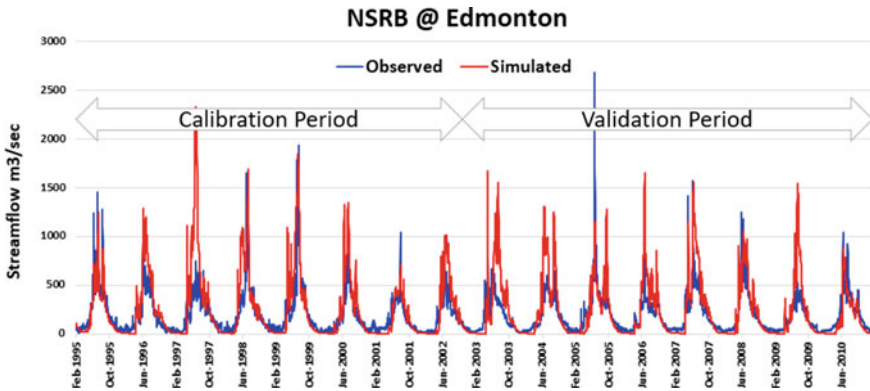


Fig. 2.27 Comparison of observed and simulated daily runoff of NSR at Edmonton for calibration (Feb 1995–Dec 2002) and validation period (Jan 2003–Dec 2010) using MESH hydrological model

and observed flows. The prediction of low flows (lnNSE) could be improved further to reduce bias. However, the overall performance of model dynamics and seasonal variability is well captured by the MESH model with a KGE value of 0.47 indicating a strong relationship between simulated and observed flows. MESH provides a close fit to the recorded flows for the calibration period, while for the independent validation period the performance is somewhat reduced, as expected in validation mode. The reduction is, however, limited, and the model is able to maintain a very good representation of the overall water balance and the inter-annual and seasonal variations. The NSE and KGE values cannot be directly compared and should not be treated as approximately equivalent (Knoben et al. 2019).

2.5.3 Streamflow Projections

The results of running the calibrated MESH model with 15 ensemble members of bias-corrected CanRCM4 (RCP 8.5) data from 1950 to 2100 are shown in Fig. 2.28. This ensemble of time series exhibits large variability around a trend of increasing flow. These results are for one ESM (CanESM2) and one RCM (CanRCM4). We have controlled for uncertainty with the use one GCM/RCM pair and one greenhouse gas emission scenario. Thus, differences among the streamflow projections reflect the internal variability of the hydroclimate in a warming climate. Figure 2.28 indicates that the future flow of the NSR will include the annual and decadal variability that is evident in our 800-year tree-ring reconstruction of the river flow. However, the range of annual flows will exceed those observed in the recent past. This very likely represents the amplification of the hydrological cycle in a warmer climate. Low flows, in particular, frequently reach those in the gauge record, even though a warming climate will be characterized by more precipitation and rising mean water levels.

Table 2.2 Goodness of fit results for the calibration and validation period of NSR at Edmonton streamflow station

Goodness of fit statistic	Calibration (Feb 1995–Dec 2002)			Validation (Jan 2003–Dec 2010)		
	Nash–Sutcliffe efficiency (NSE)	Log of Nash–Sutcliffe efficiency (lnNSE)	Kling–Gupta efficiency (KGE)	Nash–Sutcliffe efficiency (NSE)	Log of Nash–Sutcliffe efficiency (lnNSE)	Kling–Gupta efficiency (KGE)
	0.69	0.4	0.47	0.67	0.32	0.29

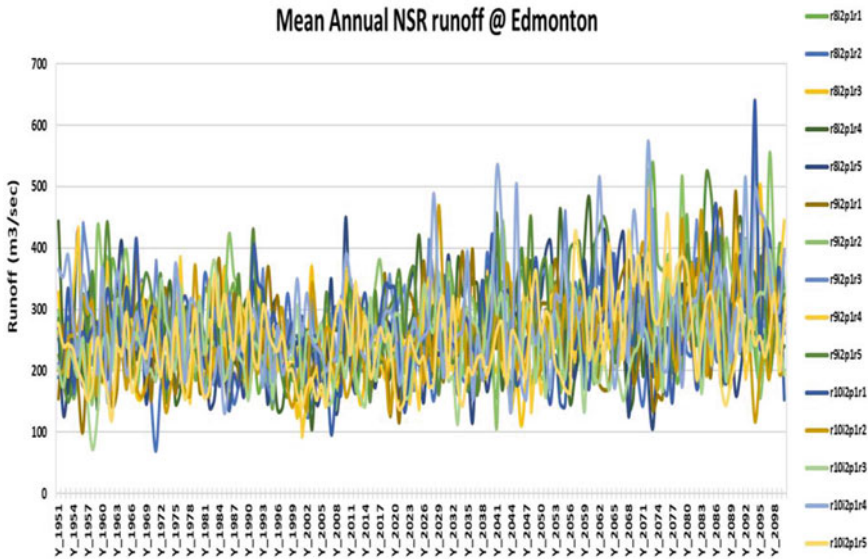


Fig. 2.28 Mean annual runoff of NSR at Edmonton using MESH and a 15-member ensemble of bias-corrected CanRCM4 data (RCP8.5)

Figure 2.29 is a plot of the annual water-year hydrograph for the baseline (1951–2010) and future periods (2041–2100). The daily flows were derived from the MESH model run with the 15-member ensemble of bias-corrected CanRCM4 data and the high emission scenario RCP 8.5. It clearly shows a shift in the hydrograph towards peak flows earlier in the year, with higher winter flows, early snowmelt and lower summer flows. There is a one-month shift towards earlier snowmelt and peak flow.

2.6 Discussion

Changes in the severity of extreme hydrological events, and in the seasonal distribution of water resources, will have major impacts on terrestrial and aquatic ecosystems and on the availability of municipal and industrial water supplies (Sturm et al. 2017; Fyfe et al. 2017). Both incremental long-term changes in water levels and extreme fluctuations around the changing baseline will have impacts requiring adaptation of water resource planning and policy. Water allocation and the design of storage and conveyance structures, such as reservoir and irrigation canals, are based mainly on average seasonal water levels, but otherwise water resources are managed to prevent the adverse impacts of flooding and drought. The operation, and possibly structural integrity, of infrastructure for drainage, water supply and treatment is vulnerable to climate change. Much of the risk is due to the expectation of more intense precipitation, prolonged low water levels and more extreme weather events.

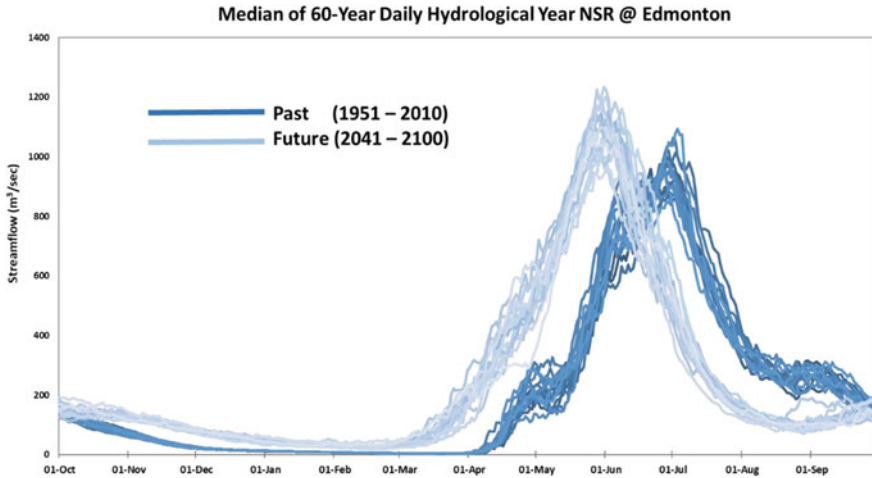


Fig. 2.29 Comparison of median 60-Year of daily NSR runoff at Edmonton for a baseline from (1951–2010) and future scenarios (2041–2100) derived from the MESH hydrological model run with the 15-member ensemble of bias-corrected CanRCM4 data and the high emission scenario RCP8.5

In this paper, we examined the implications of climate change for water security in western Canada, using the North Saskatchewan River Basin (NSRB) as a case study. We developed reconstructions of the pre-industrial streamflow and projections of future climate and hydrology. Most of the climate change in this region has been an increase in the lowest temperatures; minimum daily winter temperatures have increased by about 6 °C. There is no significant trend in the instrumental record of precipitation. Fluctuations in precipitation over the past 120 years are dominated by large differences between years and decades.

A decrease in the average flow of the North Saskatchewan River (NSR) at Edmonton since 1911 is consistent with a warming climate and the resulting loss of glacier ice and summer snowpack at high elevations in the headwaters of the river basin. However, the decline is relatively small compared to large natural inter-annual and decadal variability in flow. Natural cycles in water levels are very apparent in the paleohydrology of the NSR, an 815-year reconstruction of seasonal river flow from tree rings collected in the upper part of the river basin. The decadal cycle is particularly evident in the paleohydrology, with long periods of consistently low river levels and hydrological drought.

Future projections from RCMs suggest warmer and wetter conditions in winter and spring and, on average, drier conditions in mid to late summer. One of the most robust climate change projections is an increase in rainfall intensity. A warming climate will amplify both the wet and dry phases of the natural cycle in the regional hydroclimate. In response to the projected climate changes, the seasonal pattern of river flow will shift, with future river levels peaking about one month earlier. Cold

season (winter and early spring) flows will be significantly higher. River flows in June to August will be, on average, lower than in the past.

Our approach to research on water security examines the extent to which impacts of global climate change on water resources exceeds the natural variability in hydroclimate as captured by our tree-ring records. Proxy records of past climate and hydrology can be used to constrain future projections of regional hydroclimate (e.g. Ault et al. 2014; PAGES Hydro2k Consortium 2017; Schmidt et al. 2014; Smerdon et al. 2015). Historical model simulations and proxy records cannot be directly compared unless initial conditions are identical. Model simulation of the unforced (internal) variations, which the proxies depict, will differ among models. Therefore, the best approach to comparing paleo- and climate model data is based on their underlying statistical distributions and the full spectrum of variability. Despite uncorrelated temporal variability, the power spectra of the time series will reflect similar climate forcings, such as teleconnections between the regional climate and ocean–atmosphere oscillations. To illustrate these types of proxy-model comparisons, Fig. 2.30 is a plot of 200 years of tree-ring inferred annual normalized streamflow at Edmonton and output from the MESH hydrological model driven using precipitation and temperature from a pre-industrial control run of the CMIP6 model MRI ES M 2.0. The two curves exhibit similar inter-annual variability and range of streamflow. A wavelet transform of the winter and spring components of these time series (Fig. 2.31) reveals that they both have significant high-frequency variability corresponding to the influence of ENSO, although whereas this mode of variability spans for 2–8 years for the proxy streamflows, it is confined to a more narrow range (2–4 years) for the modelled river hydrology. Decadal scale variability is more prominent in the tree-ring record, suggesting that the climate model may not be fully simulating this significant mode of variability.

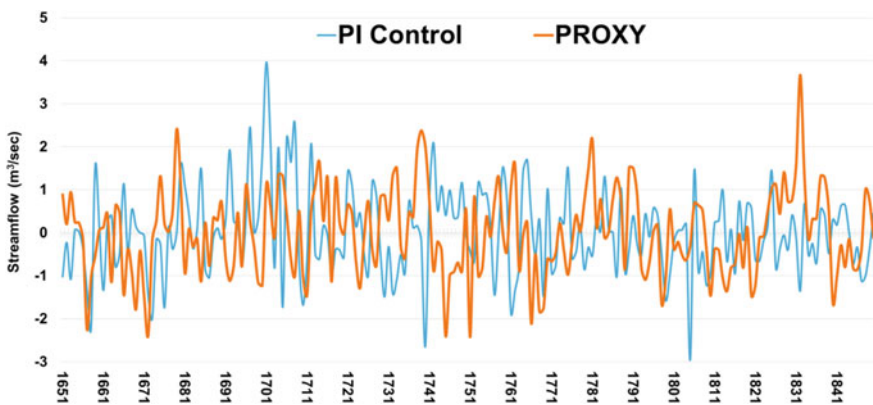


Fig. 2.30 200 years of tree-ring inferred annual normalized streamflow at Edmonton and output from the MESH hydrological model driven using precipitation and temperature from a pre-industrial control run of the CMIP6 model MRI ES M 2.0

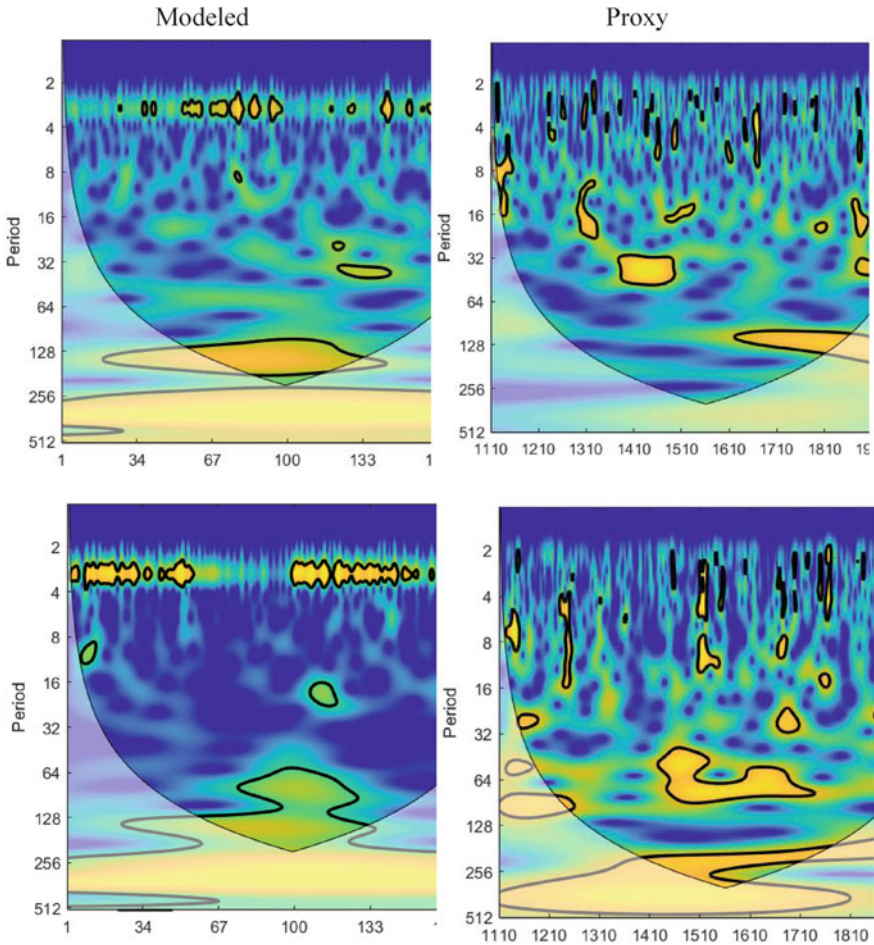


Fig. 2.31 Wavelet Transform of winter (top) and spring (bottom) modelled (left) and proxy (right) streamflow at Edmonton

As a warming climate amplifies the hydrological cycle, the range of river levels will expand, with larger departures from a shifting baseline of higher winter flows and lower summer flows. More precipitation falling as rain rather than snow, combined with earlier spring snow melt, will result in earlier peak streamflows, with subsequent reduced flows in summer, the season of highest water demand. Data from recent decades indicates that absolute water use and demand has increased but at a much lesser rate than the increasing population of the Edmonton region. As a result, there has been a decoupling of per capita water use from growth in the economy and population of the region.

Acknowledgements Funding for the research described in this paper was provided by EPCOR Utilities and the Natural Science and Engineering Council of Canada. The authors thank Mike Christensen for his comments and advice and Sheena Hatcher, Suzy Christoffel, Juan Mauricio Bedoya and Andrea Sanchez-Ponton for their assistance with field and laboratory research.

References

- Abbott BW, Bishop K, Zarnetske JP, Minaudo C, Chapin FS, Krause S et al (2019) Human domination of the global water cycle absent from depictions and perceptions. *Nat Geosci* 12. <https://doi.org/10.1038/s41561-019-0374-y>
- Adjusted and Homogenized Canadian Climate Data (AHCCD) (2017). Available online: <https://ec.gc.ca/dccha-ahccd/default.asp?lang=En&n=B1F8423>
- AMEC Earth & Environmental (2007) Current and future water use in Alberta. Prepared for Alberta Environment, Edmonton, Alberta, 724 pp
- Asong ZE, Wheeler HS, Pomeroy JW, Pietroniro A, Elshamy ME, Prinz D, Cannon A (2018) WFDEI-GEM-CaPA: A 38-year high-resolution meteorological forcing data set for land surface modeling in North America. *Earth Syst Sci Data Discuss*. <https://doi.org/10.5194/essd-2018-128>
- Asong ZE, Elshamy ME, Prinz D, Wheeler HS, Pomeroy JW, Pietroniro A, Cannon A (2020) High-resolution meteorological forcing data for hydrological modelling and climate change impact analysis in the Mackenzie River Basin. *Earth Syst Sci Data* 12:629–645. <https://doi.org/10.5194/essd-12-629-2020>
- Ault TR, Cole JE, Overpeck JT, Pederson GT, Meko DM (2014) Assessing the risk of persistent drought using climate model simulations and paleoclimate data. *J Clim* 27:7529–7549. <https://doi.org/10.1175/jcli-d-12-00282.1>
- Barrow EB, Sauchyn DJ (2019) Uncertainty in climate projections and time of emergence of climate signals in western Canada. *The Int J Climatol*. <https://doi.org/10.1002/joc.6079>
- Bawden AJ, Burn DH, Prowse TD (2015) Recent changes in patterns of western Canadian river flow and association with climatic drivers. *Hydrol Res* 46(4):551–565. <https://doi.org/10.2166/nh.2014.032>
- Bonsal BR, Peters DL, Seglenieks F, Rivera A, Berg A (2019) Changes in freshwater availability across Canada. In: Bush E, Lemmen DS (eds) Chapter 6: Canada's changing climate report. Government of Canada, Ottawa, Ontario, pp 261–342
- Burn DH, Aziz OIA, Pietroniro A (2004) A comparison of trends in hydrological variables for two watersheds in the Mackenzie River Basin. *Can Water Res J* 29(4):283–298. <https://doi.org/10.4296/cwrj283>
- Canadian Digital Elevation Model (CDEM) (2015) computer file. Natural Resources Canada, Ottawa, ON
- City of Calgary, Water Resources (2007) Water efficiency plan: 30-in-30, by 2033. Calgary, Alberta, p 80
- Comeau LEL, Pietroniro AI, Demuth MN (2009) Glacier contribution to the North and South Saskatchewan Rivers. *Hydrol Process* 23:2640–2653. <https://doi.org/10.1002/hyp.7409>
- Davison B, Pohl S, Domes P, Marsh P, Pietroniro A, MacKay M (2006) Characterizing snowmelt variability in a land-surface-hydrologic model. *Atmos Ocean* 44(3):271–287. <https://doi.org/10.3137/ao.440305>
- DeOreo WB, Mayer P, Dziegielewski B, Kiefer J (2016) Residential end uses of water, version 2: executive report for more information about this project, please visit www.waterrf.org/4309. Prepared by: Water Research Foundation, 16 pp
- Deser C, Phillips A, Bourdette V, Teng H (2012) Uncertainty in climate change projections: the role of internal variability. *Clim Dyn* 38:527–546. <https://doi.org/10.1007/s00382-010-0977>

- Environment Canada (1995) The state of Canada's climate: monitoring variability and change. SOE Report 95-1. Atmospheric Environment Service, Environment Canada, Ottawa, Canada
- EPCOR (2017) Source water protection plan. Edmonton's Drinking Water System, 138 pp
- Fye F, Stahle D, Cook E, Cleaveland M (2006) NAO influence on sub-decadal moisture variability over central North America. *Geophys Res Lett* 33:L15707
- Fyfe J, Derksen C, Mudryk L, Flato G, Santer B, Swart N, Molotch N, Zhang X, Wan H, Arora V, Scinocca J, Jiao Y (2017) Large near-term projected snowpack loss over the western United States. *Nat Commun* 8 <https://doi.org/10.1038/NCOMMS14996>
- Gizaw MS, Gan TY (2015) Possible impact of climate change on future extreme precipitation of the oldman, bow and red deer river basins of Alberta. *Int J Climatol* 36(1):208–224
- Golder Associates Ltd. (2008) Assessment of climate change effects on water yield from the North Saskatchewan River Basin
- Grasby SE, Chen Z, Hamblin AP, Wozniak PRJ, Sweet AR (2009) Regional characterization of the Paskapoo bedrock aquifer system, southern Alberta. *Can J Earth Sci* 45(12):1501–1516. <https://doi.org/10.1139/E08-069>
- Grinsted A, Moore JC, Jevrejeva S (2004) Application of the cross wavelet transform and wavelet coherence to geophysical time series. *Nonlinear Process Geophys* 11:561–566. <https://doi.org/10.5194/npg-11-561-2004>
- Gurrapu S, St-Jacques J-M, Sauchyn DJ, Hodder KH (2016) The influence of the PDO and ENSO on the annual flood frequency of Southwestern Canadian Prairie Rivers. *J Am Water Resour Assoc* 52(5):1031–1045
- Hawkins E, Sutton R (2009) The potential to narrow uncertainty in regional climate predictions. *Bull Am Meteorol Soc* 90(8):1095–1108. <https://doi.org/10.1175/2009BAMS2607.1>
- Hayashi M, Farrow CR (2014) Watershed-scale response of groundwater recharge to inter-annual and inter-decadal variability in precipitation (Alberta, Canada). *Hydrogeol J* 22(8):1825–1839
- Howard IM, Stahle DW, Feng S (2019) Separate tree-ring reconstructions of spring and summer moisture in the northern and southern Great Plains. *Clim Dyn* 52:5877–5897
- Hughes AT, Smerdon BD, Alessi DS (2017) Hydraulic properties of the Paskapoo formation in west-central Alberta. *Can J Earth Sci* 54(8):883–892
- IPCC (2014) Climate change 2014: synthesis report. Contribution of working groups I, II and III to the fifth assessment report of the intergovernmental panel on climate change. In: Pachauri, RK, Meyer LA (eds) Core writing team. IPCC, Geneva, Switzerland, 151 pp
- Jiang R, Gan TY, Xie J, Wang N, Kuo CC (2017) Historical and potential changes of precipitation and temperature of Alberta subjected to climate change impact: 1900–2100. *Theoret Appl Climatol* 127(3–4):725–739
- Jiménez Cisneros BE, Oki T, Arnell NW, Benito G, Cogley JG, Döll P et al (2014) Freshwater resources. In: Field CB, Barros VR, Dokken DJ, Mach KJ, Mastrandrea MD, Bilir TE et al (eds) Climate change 2014: impacts, adaptation, and vulnerability. Part A: global and sectoral aspects. Contribution of working group II to the fifth assessment report of the intergovernmental panel of climate change
- Kerr SA, Andreichuk Y, Christoffel S, Sauchyn DJ (In review). Comparing paleo reconstructions of warm and cool season streamflow (1400–2018) for the North and South Saskatchewan River Sub-basins, Western Canada. *Can Water Resour J*
- Kienzle SW, Nemeth MW, Byrne JM, MacDonald RJ (2012) Simulating the hydrological impacts of climate change in the upper North Saskatchewan River basin. *J Hydrol* 412–413:76–89
- Knoben WJM, Freer JE, Woods RA (2019) Technical note: inherent benchmark or not? Comparing Nash-Sutcliffe and Kling-Gupta efficiency scores. *Hydrol Earth Syst Sci* 23:4323–4331. <https://doi.org/10.5194/hess-23-4323-2019>
- Kouwen N, Soulis ED, Pietroniro A, Donald J, Harrington RA (1993) Grouped response units for distributed hydrologic modelling. *J Water Resour Plan Manage* 119(3):289–305
- Liu H, Davies E (2019) Municipal water demand forecasting with ANN and SD models under climate change. In: Proceedings of the 8th international conference on water resources and environment research, ICWRER 2019, June 14th—18th, 2019, Hohai University, Nanjing, China.

- MacDonald RJ, Byrne JM, Boon S, Kienzle SW (2012) Modelling the potential impacts of climate change on snowpack in the North Saskatchewan River Watershed. *Water Resour Manage* 26:3053–3076. <https://doi.org/10.1007/s11269-012-0016-2>
- Marshall SJ, White EC, Demuth MN, Bolch T, Wheate R, Menounos B, Beedle MJ, Shea JM (2011) Glacier water resources on the eastern slopes of the Canadian Rocky mountains. *Can Water Resour J* 36(2):109–134. <https://doi.org/10.4296/cwrj3602823>
- Marvel K, Cook BI, Bonfils C et al (2019) Twentieth-century hydroclimate changes consistent with human influence. *Nature* 569:59–65. <https://doi.org/10.1038/s41586-019-1149-8>
- Meko DM, Woodhouse CA, Morino K (2012) Dendrochronology and Links to Streamflow. *J Hydrol* 412–413:200–209. <https://doi.org/10.1016/j.jhydrol.2010.11.041>
- Mekonnen MA, Wheeler HS, Ireson AM, Spence C, Davison B, Pietroniro A (2014) Towards an improved land surface scheme for prairie landscapes. *J Hydrol* 511:105–116. <https://doi.org/10.1016/j.jhydrol.2014.01.020>
- Moore RD, Allen DM, Stahl K (2007) Climate change and low flows: influences of groundwater and glaciers. Final report prepared for Climate Change Action Fund, Natural Resources Canada, Vancouver, BC
- Mudryk LR, Derksen C, Howell S, Laliberté F, Thackeray C, Sospedra-Alfonso R, Vionnet V, Kushner PJ, Brown R (2018) Canadian snow and sea ice: historical trends and projections. *The Cryosphere* 12:1157–1176. <https://doi.org/10.5194/tc-12-1157-2018>
- North Saskatchewan Watershed Alliance (NSWA) (2012) Atlas of the North Saskatchewan River Watershed in Alberta. The North Saskatchewan Watershed Alliance Society, Edmonton, Alberta
- North Saskatchewan Watershed Alliance (NSWA) (2014) Preliminary steps for the assessment of instream flow needs in the North Saskatchewan River Basin. Edmonton, Alberta
- PAGES Hydro2k Consortium (2017) Comparing proxy and model estimates of hydroclimate variability and change over the Common Era. *Clim Past* 13:1851–1900. <https://doi.org/10.5194/cp-13-1851-2017>
- Perez-Valdivia C, Sauchyn D (2012) Groundwater levels and teleconnection patterns in the Canadian Prairies. *Water Resour Res* 48(W07516):2012. <https://doi.org/10.1029/2011WR010930>
- Pietroniro A, Soulis E (2003) A hydrology modelling framework for the Mackenzie GEWEX programme. *Hydrol Process* 17(3):673–676
- Pietroniro A, Fortin V, Kouwen N, Neal C, Turcotte R, Davison B, Versegny D, Soulis ED, Caldwell R, Evora N, Pellerin P (2007) Development of the MESH modelling system for hydrological ensemble forecasting of the Laurentian Great Lakes at the regional scale. *Hydrol Earth Syst Sci* 11:1279–1294. <https://doi.org/10.5194/hess-11-1279-2007>
- Pomeroy J, Stewart RE, Whitfield PH (2005) The 2013 flood event in the Bow and Oldman River basins: causes, assessment, and damages. *Can Water Resour J*
- Pouliot D, Latifovic R, Olthof I (2017) Development of a 30 m spatial resolution land cover of Canada: contribution to the harmonized North America Land Cover Dataset, 11–15 Dec, AGU Fall Meeting 2017
- Rood SB, Samuelson GM, Weber JK, Wywrot KA (2005) Twentieth-century decline in streamflows from the hydrographic apex of North America. *J Hydrol* 306(1–4):215–233. <https://doi.org/10.1016/j.jhydrol.2004.09.010>
- Sauchyn D, Ilich N (2017) Nine hundred years of weekly streamflows: stochastic downscaling of ensemble tree-ring reconstructions. *Water Resour Res* 53:9266–9283. <https://doi.org/10.1002/2017WR021585>
- Sauchyn D, Vanstone J, Perez-Valdivia C (2011) Modes and forcing of hydroclimatic variability in the Upper North Saskatchewan River Basin since 1063. *Can Water Resour J* 36(3):205–217
- Sauchyn DJ, Vanstone J, St. Jacques JM, Sauchyn R (2015) Dendrohydrology in Canada's western interior and applications to water resource management. *J Hydrol* 529:548–558
- Schmidt GA et al (2014) Using palaeo-climate comparisons to constrain future projections in CMIP5. *Clim Past* 10:221–250. <https://doi.org/10.5194/cp-10-221-2014>
- Scinocca JF, Kharin VV, Jiao Y, Qian MW, Lazare M, Solheim L, Dugas B (2016) Coordinated global and regional climate modelling. *J Clim* 29:17–35. <https://doi.org/10.1175/JCLI-D-15-0161.1>

- Smerdon JE, Cook BI, Cook ER, Seager R (2015) Bridging past and future climate across paleoclimatic reconstructions, observations, and models: a hydroclimate case study. *J Clim* 28:3212–3231. <https://doi.org/10.1175/jcli-d-14-00417.1>
- Soulis ED, Snelgrove KR, Kouwen N, Seglenieks F, Verseghy DL (2000) Towards closing the vertical water balance in Canadian atmospheric models: coupling of the land surface scheme CLASS with the distributed hydrological model watflood. *Atmos Ocean* 38(1):251–269. <https://doi.org/10.1080/07055900.2000.9649648>
- St. Jacques J-M, Sauchyn DJ, Zhao Y (2010) Northern Rocky Mountain streamflow records: global warming trends, human impacts or natural variability? *Geophys Res Lett* 37(6)
- St. Jacques JM, Huang YA, Zhao Y, Lapp SL, Sauchyn DJ (2014) Detection and attribution of variability and trends in streamflow records from the Canadian Prairie Provinces. *Canad Water Resour J* 39(3):270–284. <https://doi.org/10.1080/07011784.2014.942575>
- Stahle DW, Cook ER, Burnette DJ, Torbenson MCA, Howard IM, Griffin D, Villanueva JV, Cook BI, Williams PA, Watson E, Sauchyn DJ, Pederson N, Woodhouse CA, Pederson GT, Meko DM, Coulthard B, Crawford CJ (2020) Dynamics, variability, and change in seasonal precipitation reconstructions for North America. *J Clim* 33:3173–3195
- Sturm M, Goldstein M, Parr C (2017) Water and life from snow: a trillion-dollar science question. *Water Resour Res* 53:3534–3544. <https://doi.org/10.1002/2017WR020840>
- Szeto K, Zhang X, White ER, Brimelow J (2016) The 2015 extreme drought in Western Canada. Explaining extreme events of 2015 from a climate perspective. In: Herring S et al (eds) Chapter 9, Special Supplement to the Bulletin of the American Meteorological Society, vol 97, no 12
- Tam BY, Szeto K, Bonsal B, Flato G, Cannon AJ, Rong R (2018) CMIP5 drought projections in Canada based on the standardized precipitation evapotranspiration index. *Can Water Resour J/Revue Canadienne Des Ressources Hydriques*. <https://doi.org/10.1080/07011784.2018.1537812>
- Tennant C, Menounos B (2013) Glacier change of the Columbia Icefield, Canadian Rocky Mountains, 1919–2009. *J Glaciol* 59(216):671–686. <https://doi.org/10.3189/2013JoG12J135>
- Teufel B, Diro GT, Whan KM, Jeong DI, Ganji A, Huzly O, Winger K, Gyakum JR, de Elia R, Zwiers FW, Sushama L (2017) Investigation of the 2013 Alberta flood from weather and climate Perspectives. *Clim Dyn* 48:2881
- Thompson J (2016) An update on water allocation and use in the North Saskatchewan River Basin in Alberta. Available at: <https://www.saskriverbasin.ca/images/files/Water%20Use%20Update-John%20Thompson.pdf>
- Treasury Board and Finance (2018) Office of Statistics and Information – Demography, Population Project, Alberta and Census Divisions 2018–2046, July 3
- Vaghefi SA, Sauchyn DJ, Andreichuk Y, Irvani M, Goss GG, Faramarzi M (2019) Regionalization and parameterization of a hydrologic model significantly affect the cascade of uncertainty in climate-impact projections. *Clim Dyn* 1–26. <https://doi.org/10.1007/s00382-019-04664-w>
- Verseghy D (1991) Class—a Canadian land surface scheme for GCMS. I. Soil model. *Int J Climatol* 11(2):111–133. <https://doi.org/10.1002/joc.3370110202>
- Verseghy D, McFarlane NA, Lazare M (1993) CLASS—a Canadian land surface scheme for GCMs. II. Vegetation model and coupled runs. *Int J Climatol* 13(4):347–370. <https://doi.org/10.1002/joc.3370130402>
- Vincent LA, Wang XL, Milewska EJ, Wan H, Yang F, Swail V (2012) A second generation of homogenized Canadian monthly surface air temperature for climate trend analysis. *J Geophys Res* 117:D18110. <https://doi.org/10.1029/2012JD017859>
- Worley Parsons (2009) North Saskatchewan River Basin overview of groundwater conditions, issues, and challenges.
- Zhang X, Flato G, Kirchmeier-Young M, Vincent L, Wan H, Wang X, Rong R, Fyfe J, Li G, Khari VV (2019) Changes in temperature and precipitation across Canada. In: Bush E, Lemmen DS (eds), Chapter 4, Canada’s changing climate report. Government of Canada, Ottawa, Ontario